Chemical Engineering Journal 156 (2010) 200–205

Contents lists available at ScienceDirect

Chemical Engineering Journal

journal homepage: www.elsevier.com/locate/cej

Characterization of silica-coated silver nanoparticles prepared by a reverse micelle and hydrolysis–condensation process

Nobuhiro Hagura[a], W. Widiyastuti[b], Ferry Iskandar[a], Kikuo Okuyama[a,*]

[a] Department of Chemical Engineering, Graduate School of Engineering, Hiroshima University, 1-4-1 Kagamiyama, Higashi-Hiroshima 739-8527, Hiroshima, Japan
[b] Department of Chemical Engineering, Faculty of Industrial Technology, Institut Teknologi Sepuluh Nopember (ITS), Kampus ITS Keputih-Sukolilo, Surabaya 60111, Indonesia

ARTICLE INFO

Article history:
Received 4 August 2009
Received in revised form
24 September 2009
Accepted 6 October 2009

Keywords:
Silica coating
Microemulsion
Hydrolysis reaction rate
Surface plasmon resonance (SPR)

ABSTRACT

Described herein is the synthesis of individually silica-coated silver nanoparticles using a reverse micelle method followed by hydrolysis and condensation of tetraethoxysilane (TEOS). The size of a silica-coated silver nanoparticle can be controlled by changing the reaction time and the concentration of TEOS. By maintaining the size of a silver nanoparticle as a core particle at around 7 nm, the size of a silica-coated silver nanoparticle increased from 13 to 28 nm as the reaction time increased from 1 to 9 h due to an increase in silica thickness. The size of silica-coated silver nanoparticles also increased from 15 to 22 nm as the TEOS concentration increased from 7.8 to 40 mM. The size of a silica-coated silver nanoparticle can be accurately predicted using the rate of the hydrolysis reaction for TEOS. Neither the dispersion nor the film of silica-coated silver nanoparticles exhibited any peak shifting during surface plasmon resonance (SPR) at around 410 nm, whereas, without silica coating, the SPR peak of Ag film shifted to 466 nm.

1. Introduction

It is well known that nanoparticles exhibit great properties that differ remarkably from their bulk materials. They are used in many applications: microelectronic materials, chemical and mechanical industries, and pharmaceutical and biomaterial production [1]. However, nanoparticles either in powder or colloid form tend to agglomerate and form larger particles when they are aged over a few days resulting in the degradation of their characteristics. An attempt has been made to maintain un-agglomerated nanoparticles by individually coating the metal nanoparticles called core–shell nanoparticles. The shell also functions to prevent the degradation of characteristic performance caused by the agglomeration process and to control the distance between core particles by adjusting the shell thickness of core–shell particles. Moreover, core–shell nanoparticles may exhibit unique characteristics and the properties of the core can be altered. As a shell material, silica is preferred because it is easy to control the deposition process, chemical inertness, and optical transparency in the visible range [2–4]. Silver nanoparticles and silica-coated silver nanoparticles are both of interest because their surface plasmon resonance (SPR) characterizes both linear and nonlinear optical properties [5,6].

It is common to prepare a colloid of metal nanoparticles prior to the silica coating process. Among preparation methods for silver nanoparticles – chemical reduction, photochemical, electrochemical, and biochemical – the microemulsion or micelle method has advantages such as uniform shape and size-controllable particles [7]. The use of oleylamine as both a reducing agent by thermal decomposition and a monolayer protective agent has been reported by previous investigators in the production of monodispersed functional nanoparticles such as gold, silver and magnetite [8–10]. Better control of the size and size distribution of silver nanoparticles, as well as a reduction mechanism for the silver ion, has been reported with use of the oleylamine–liquid paraffin system [11]. This method has promise for the large-scale synthesis of organoamine-protected nanoparticles, because it is inexpensive, versatile, and very reproducible. We used this method to produce silver nanoparticles prior to coating them with silica [6].

The preparation of silica-coated silver nanoparticles has been reported by previous investigators and summarized by Liz-Marzan and Mulvaney [2]. Giersig and co-workers reported a gold and silver colloid being coated with silica using a silane coupling agent, but the silica thickness was only approximately 2–4 nm after a 24-h reaction time [3,12]. The Stöber method is a common method used to prepare silica as shells wherein the reaction is a base-catalyzed hydrolysis of tetraethoxysilane (TEOS) followed by condensation to form silica particles [13]. In the case of silica-coated iron oxide, no pretreatment is required to promote deposition and adhesion of silica because the iron oxide particle surface has a strong affinity toward silica [14]. On the other hand, silver and gold nanoparticles tend to flocculate when the Stöber method is applied directly because of their low affinity for silica. Liz-Marzan and Philipse coated gold nanoparticles with octadecyl chains that dissolved in

* Corresponding author. Tel.: +81 82 4247716; fax: +81 82 4247850.
E-mail address: okuyama@hiroshima-u.ac.jp (K. Okuyama).

1385-8947/$ – see front matter © 2009 Elsevier B.V. All rights reserved.
doi:10.1016/j.cej.2009.10.024

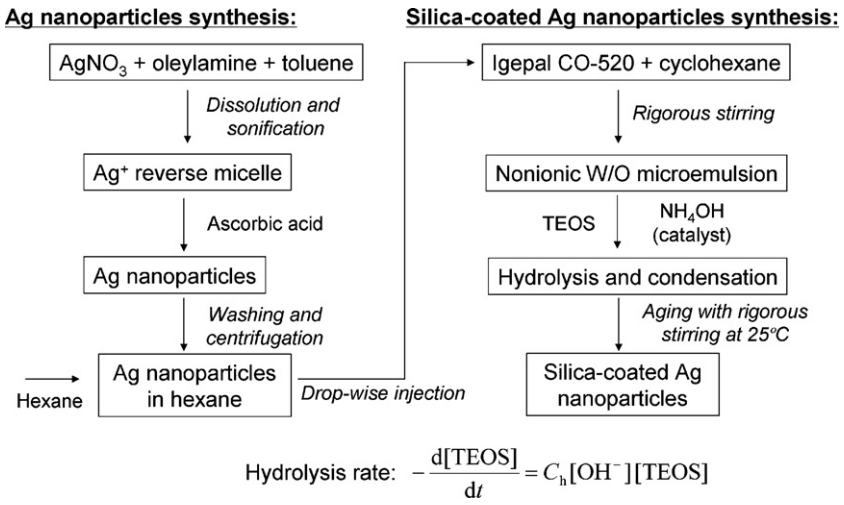

Fig. 1. Preparation procedure for silica-coated silver nanoparticles by reverse micelle and hydrolysis–condensation methods.

organic solvent and used Ludox hydrosol as silica seed before they were reacted with TEOS by Stöber synthesis for silica growth [15]. However, most gold nanoparticles are not coated by silica, and agglomerations between silica particles can be observed. Kobayashi et al. prepared silica-coated silver nanoparticles using borohydride as a reduction agent and silica as a coating material with the modified Stöber method [16]. They used dimethylamine (DMA) to obtain a proper coating of silica onto silver nanoparticles. The shell thickness can be controlled by varying the concentration of TEOS. Another modified Stöber method applied by our group involved the injection of silver nanoparticles into hexadecyltrimethyl ammonium bromide (HTAB) dissolved in de-ionized water before coating by TEOS [6]. Most silver nanoparticles coated by mesoporous silica were generated using this method. However, the agglomeration of silver nanoparticles as a core material persisted when using this method.

The use of a non-ionic surfactant such as Igepal CO-520 to obtain more dispersed colloidal nanoparticles has been reported. A reverse microemulsion method that uses Igepal CO-520 as a surfactant has been reported in the synthesis of silica-coated gold and silver nanoparticles using hydrazine hydrate as a reduction agent [17]. This method also has been reported in the synthesis of silica-coated gold nanoparticles using oleylamine to stabilize the gold nanoparticles prior to the coating process [18]. The effect of structure in the formation of silica nanoparticles using a hydrolysis reaction and condensation of TEOS in nonionic water-in-oil microemulsion was characterized by Chang and Fogler [19]. Three types of nonionic surfactants, including Igepal CO-520 and two types of oils (heptane and cyclohexane), were used for comparison. From the results, the silica reacting species in Igepal CO-520 microemulsion led to the most consumption of TEOS among surfactants. Therefore, a change in the size of silica might be accurately predicted in this synthesis method.

For the present study, we combined methods from several groups based on the advantages offered for control in the preparation of silica-coated silver nanoparticles. We used three consecutive methods to prepare these particles: the preparation of colloidal silver nanoparticles, a silica-coated silver process, and the selection of a surfactant as a surface modification during the coating process. Oleylamine and ascorbic acid were used as a surfactant and a reduction agent, respectively, of silver nitrate in the synthesis of silver nanoparticles. Igepal CO-520 was selected as a surfactant for the synthesis of silica-coated silver nanoparticles during the hydrolysis reaction and condensation of TEOS. The particle morphology and the thickness of the silica shell were controlled by controlling the reaction time and the TEOS concentration. These experimental results were compared to the theoretical approach by applying the rate of the hydrolysis reaction of TEOS to the calculation to predict the thickness of silica coating. In addition, the optical absorbance spectra of silver nanoparticles and silica-coated silver nanoparticles, both dispersed in liquid medium and film, were evaluated to characterize their surface plasmon resonance (SPR).

2. Experiment

A schematic of the particle preparation and an illustration of the formation mechanism for silica-coated silver nanoparticles are outlined in Figs. 1 and 2, respectively. The preparation of silver nanoparticles as a core material of silica-coated silver nanoparticle preparation was described briefly in our previous paper [6]. Silver nitrate ($AgNO_3$, purity >99.8%, Kanto Chemical Co.), cis-9-octadecenylamine (oleylamine, $(CH_3(CH_2)_7CH{=}CH(CH_2)_8NH_2$, purity >40%, Tokyo Chemical Industry Co., Ltd.), L-ascorbic acid ($C_6H_8O_6$, purity >99.5%, Yoneyama Yakuhin Kogyo Co., Ltd.), toluene (C_6H_5–CH_3, purity >99.8%, Aldrich Chemical Co.), and *n*-hexane (C_6H_{14}, purity >95%, Wako Pure Chemical Industries Ltd.) were used to prepare silver nanoparticles. These chemicals were used as received.

A solution for microemulsion preparation was prepared by dissolving 7.8 g of nonionic surfactant: polyoxyethylene (5) nonylphenyl ether (Igepal®CO-520, 4-$(C_9H_{19})C_6H_4(OCH_2CH_2)_nOH$, $n \sim 5$, purity >99.5%, Aldrich Chemical Co.) into 170 mL of cyclohexane (C_6H_{12}, purity >99.5%, Kanto Chemical Co.). Then, silver nanoparticles dispersed in hexane were dropwise injected into the solution with vigorous stirring. After that, 2.6–40 mM of TEOS and 0.006 vol% of ammonium hydroxide (NH_4OH solution, 28–30 vol%, Kanto Chemical Co.) was added into the microemulsion, respectively. Ammonium hydroxide was used to accelerate the hydrolysis reaction of TEOS. The reaction was stirred vigorously for 1–9 h, and the temperature was maintained at 25 °C. Silica-coated silver nanoparticles were obtained by centrifugation at 10000 rpm using ethanol as a solvent.

In order to investigate the effect of reaction time on silica shell thickness, 26 mM of TEOS was maintained. The reaction time was varied by 1, 3, 5, 7, and 9 h. The effect of TEOS concentration was also investigated by maintaining a reaction time of 5 h. TEOS concentration was varied by 7.9, 18.4, 29, and 40 mM. A theoretical approach was also proposed for a comparison with the experimental work. In order to ensure reproducibility, we conducted the experiment 2–3 times, which resulted in ignored deviation data.

The particle morphology was observed using field-emission scanning electron microscopy (FE-SEM, S-5000, Hitachi, Japan) operated at 20 kV. To observe the inner structure of the generated particles, a transmission electron microscopy (FE-TEM, JEM-3000F, JEOL, Japan) operated at 300 kV was used. Particle size, d_n, and the coefficient of variation, C_v, were determined from TEM images using the following equations:

$$d_n = \frac{\sum n_i d_i}{\sum n_i} \quad (1)$$

$$C_v = \frac{\left[\sum (d_i - d_n)^2 / \sum n_i\right]^{0.5}}{d_n} \quad (2)$$

To prepare silica-coated silver nanoparticle film with a thickness of 721 nm and a standard deviation of 5.4%, the prepared silica-coated silver nanoparticle colloid was deposited on a pre-cleaned glass substrate using a dip-coating method at a fixed temperature of 80 °C. Un-coated silver nanoparticle film with a thickness of 1 μm was also prepared using a spin-coating method at room temperature, which is a method of silver monolayer film preparation previously described by our group [20], for comparison of optical property performance with silica-coated silver nanoparticles dispersed in a liquid medium. The optical property was analyzed using UV–vis spectroscopy (UV-3150, Shimadzu, Japan) to measure the extinction spectra of silver nanoparticles dispersed in hexane, silver nanoparticle film, silica-coated silver nanoparticles dispersed in ethanol, and silica-coated silver nanoparticle film.

3. Results and discussion

3.1. Effect of reaction time on morphology and size of silica-coated silver nanoparticles

Fig. 3a–e shows the TEM images of silica-coated silver nanoparticles during the coating process at reaction times of 1, 3, 5, 7 and 9 h, respectively, by fixing a TEOS concentration of 26 mM. The size increased from 13.3 to 25.2 nm as the reaction time increased from 1 to 9 h with a coefficient of variation of 6.7–14.1%. For a reaction time of 1 h, agglomeration between nanoparticles is shown in Fig. 3a. A reaction time of 1 h was too short to generate un-agglomerated particles. For a reaction time of 3–9 h, un-agglomerated silica-coated silver nanoparticles are shown in Fig. 3b–e.

The percentages of silica nanoparticles containing silver nanoparticles as a core particle for reaction times of 1, 3, 5, 7, and 9 h were 81, 82, 89, 79, and 77%, respectively. For silica-coated silver nanoparticles produced with reaction times of 1, 3, 5, 7, and 9 h, the average diameters of the silver nanoparticle cores were 7.6, 6.8, 6.8, 6.9, and 7.8 nm, respectively, with a coefficient of variant in the range 16.8–39.7%. Therefore, the size of the silver nanoparticles was relatively independent of the coating reaction time. Therefore, the size of the silver nanoparticles can be assumed to be independent of the coating reaction time. The size of the core particles remained constant, similar to the as-prepared silver nanoparticles, as shown in the TEM image in Fig. 3f. The reaction time affected only the shell thickness of the silica coating on the silver nanoparticles, which increased as reaction time increased. The thickness of the coated silica increased from 3.2 to 10.7 nm as the reaction time increased from 1 to 9 h.

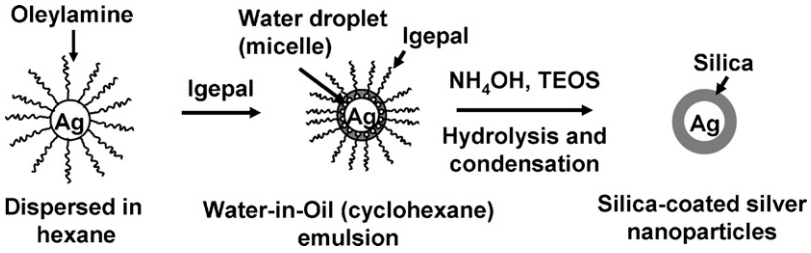

Fig. 2. Illustration of the process of silica-coated silver nanoparticles by reverse micelle and hydrolysis–condensation methods.

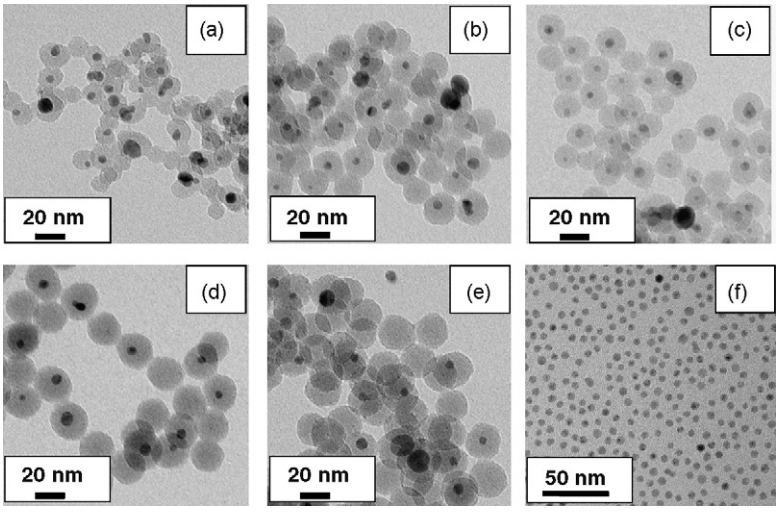

Fig. 3. TEM images of the silica-coated silver nanoparticles synthesized at various reaction times of TEOS hydrolysis, as follows: (a) 1 h, (b) 3 h, (c) 5 h, (d) 7 h, and (e) 9 h. (f) TEM image of as-prepared silver nanoparticles.

In the microemulsion system for silica particle preparation, the particle size was affected by the rate of the conversion reaction of TEOS into an active monomeric reacting species as well as by the hydrolysis reaction of TEOS prior to polymerization [19]. By applying this theory, the size of silica-coated silver nanoparticles can be predicted by assuming the core Ag particle diameter will remain constant at 7 nm during the coating process. The reaction rate for the hydrolysis of TEOS is proportional to its concentration, [TEOS], and to the concentration of hydroxyl ion in the solution, $[OH^-]$ [21]:

$$-\frac{d[\mathrm{TEOS}]}{dt} = C_h[OH^-]\,[\mathrm{TEOS}] \tag{3}$$

where C_h is the hydrolysis constant that is equal to 0.21 $m^3/(mol\,s)$ obtained from experimental data [21]. $[OH^-]$ is calculated by:

$$[OH^-] = \sqrt{K_b[NH_4OH]} \tag{4}$$

where K_b is the association constant of a weak base of ammonium hydroxide ($pK_b = 7.3$ in ethanol–water system) [21]. By assuming that the concentration of ammonium hydroxide, $[NH_4OH]$, is constant, the integration of Eq. (3) gives the following:

$$\int_{[\mathrm{TEOS}]_0}^{[\mathrm{TEOS}]} \frac{d[\mathrm{TEOS}]}{[\mathrm{TEOS}]} = \ln\frac{[\mathrm{TEOS}]}{[\mathrm{TEOS}]_0} = -C_h[OH^-]\int_0^t dt \tag{5}$$

$[\mathrm{TEOS}]_0$ is the initial concentration of TEOS that is used in the beginning reaction of hydrolysis and condensation of TEOS at $t = 0$ h. The concentration of the generated silica, $[SiO_2]$, can be solved using the following equation:

$$[SiO_2] = [\mathrm{TEOS}]_0\ \exp(-C_h[OH^-]\,t) \tag{6}$$

A simple method to obtain the number of the generated silver nanoparticles, N, is accomplished by selecting one condition of experimental data that is at $t = 1$ h by assuming the theoretical particle size is equal to the measured particle size. The number of generated silver nanoparticles, N, was the same for other conditions because the synthesis condition of silver nanoparticles was fixed. Therefore, the diameter of core–shell nanoparticles at a specified reaction time, $d_{Ag@SiO_2}$, can be calculated using the following equation:

$$d_{Ag@SiO_2} = \left[\frac{6}{\pi}\left(\frac{\pi}{6}d_{Ag}^3 + \frac{[SiO_2]Mw_{SiO_2}V_{solution}}{\rho_{SiO_2}N}\right)\right]^{1/3} \tag{7}$$

where d_{Ag} is the core diameter of silver nanoparticles, $V_{solution}$ is the total volume of the solution, Mw_{SiO_2} is the molecular weight of silica, and ρ_{SiO_2} is the density of silica. The measurement was in good agreement with the calculation of the size of silica-coated silver nanoparticles, as shown in Fig. 4. The supposed nucleation and growth kinetic of silica formation does not include silver nanoparticles, $d_{Ag} = 0$, the size of silica nanoparticles is indicated by the

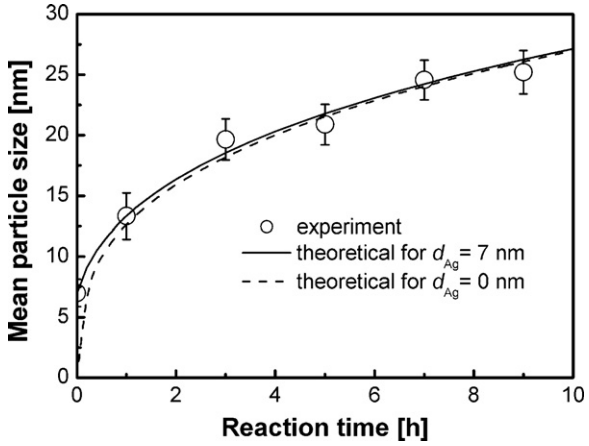

Fig. 4. Effect of hydrolysis reaction time for the silica coating process on mean particle diameter measured from TEM images and calculated theoretically.

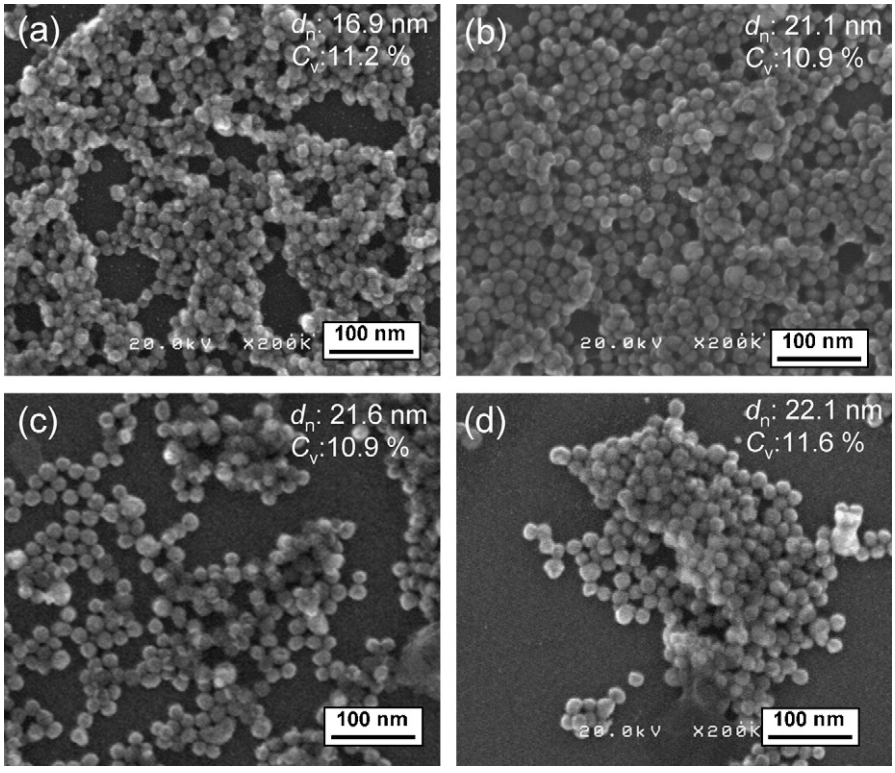

Fig. 5. FE-SEM images of silica-coated silver nanoparticles at TEOS various concentrations: (a) 7.9 mM, (b) 18.4 mM, (c) 29 mM and (d) 40 mM.

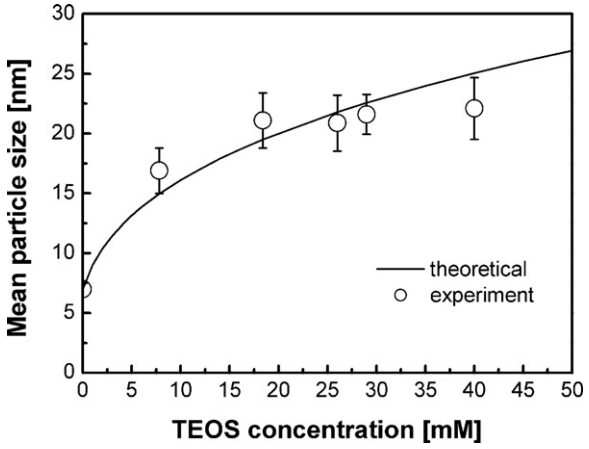

Fig. 6. Effect of TEOS concentration for the silica-coating process on mean particle diameter, as measured from FE-SEM images and calculated theoretically.

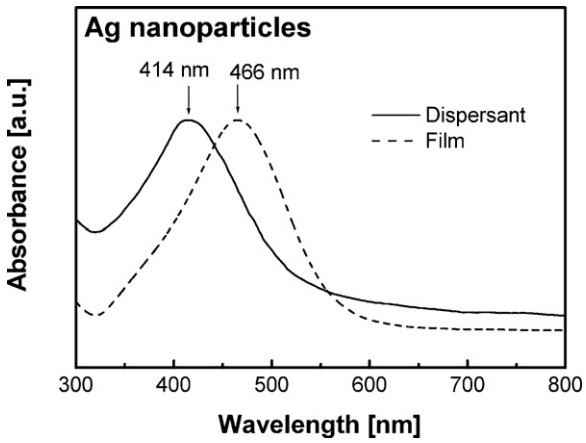

Fig. 7. Optical absorbance spectra of silver nanoparticles dispersed in a liquid medium and in film.

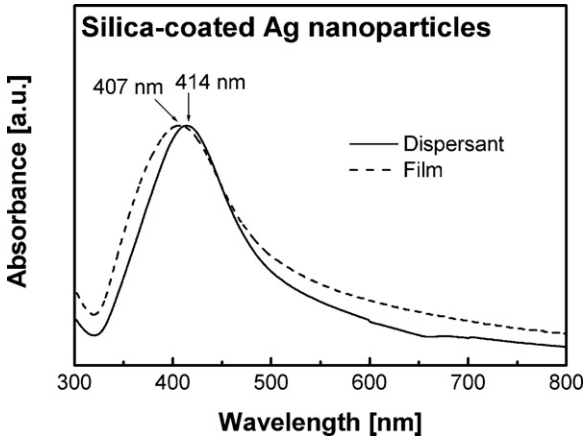

Fig. 8. Optical absorbance spectra of silica-coated silver nanoparticles dispersed in a liquid medium and in film.

dashed line in Fig. 4. This shows that the size of silica nanoparticles is similar to that of silica-coated silver nanoparticles when hydrolysis time is increased. The difference is less than 1% when hydrolysis time is greater than 5 h.

3.2. Effect of TEOS concentration as a silica source

To investigate the effect of TEOS concentration, the hydrolysis reaction was maintained for 5 h. Other conditions were also fixed. Fig. 5a–d shows the SEM images of silica-coated silver nanoparticles when TEOS concentrations were varied by 7.9, 18.4, 29, and 40 mM, respectively. The size of core–shell nanoparticles increased from 16.9 to 22.1 nm as TEOS concentration increased from 7.8 to 40 mM with a coefficient of variation of 10.9–11.6%.

The particle-size comparison for measured and theoretical calculation is shown in Fig. 6. The prediction was lower than the measurement at a lower TEOS concentration. At a higher TEOS concentration, however, the calculation result was higher than the measurement. Ammonium hydroxide might be consumed less at a lower TEOS concentration than it is at a higher TEOS concentration during the hydrolysis process. As a result, hydroxyl ion concentration is higher at a lower TEOS concentration and produces a larger particle size. A change in pH during the process caused by the change of hydroxyl ion concentration can be hindered by using the buffer solution [21] and might result a better agreement between the measurement and the calculation. In addition, size is not controlled only by the nucleation and growth kinetic of TEOS, but also by the efficacy of the capping agents in preventing Ostward ripening and coalescence [2]. This is one reason that our results agreed with our evaluations for the effect of reaction time, but there was a slight discrepancy in evaluation of the effect of TEOS concentration. This might be caused by the initial TEOS concentration dependence on the concentration of the capping agent.

3.3. Optical properties of silver nanoparticles and silica-coated silver nanoparticles dispersed in liquid medium and solid film

Fig. 7 shows the absorption spectra of silver nanoparticles without silica coating in dispersed media and film, as measured using a UV–vis spectrophotometer. The spectra of dispersed silver nanoparticles showed a broad peak of surface plasmon resonance (SPR) at a wavelength of 414 nm. However, the peak of absorption spectra shifted to a wavelength at 466 nm when the silver nanoparticle film was characterized. Without silica coating, metal nanoparticles tend to coagulate as a result of their instability [22]. Silver nanoparticle film might lose its stability rather than being dispersed in a liquid medium, which would result in the SPR characteristic change.

The peak of the absorption spectra for silica-coated silver nanoparticles, both in dispersant and film, was at wavelengths of 414 and 407 nm, respectively, as depicted in Fig. 8. In our previous investigation, similar results were obtained for the SPR characteristic of a silica-coated silver nanoparticle dispersant at a wavelength of 410 nm, which led to the conclusion that the peak of the SPR characteristic is slightly affected by the silica shell thickness [6]. Due to the increase in the shell thickness, a slight shifting of the SPR peak was also observed in silica-coated gold nanoparticles [23]. In the present study, the ratio of the core diameter and the shell thickness was 0.9 on average, which indicates that the shifted wavelength can be ignored when compared with a ratio of 3–12 that gives a span in the range of 300 nm in wavelength [24]. The shell thickness affected only the intensity of the SPR characteristic that increased with the silica shell thickness. The intense band centered at a wavelength of 407 nm was also observed for silver clusters of 6–7 nm that were well separated and homogenously distributed inside the silica matrix [25]. The same intensity of SPR peaks for silica-coated silver nanoparticle film at a wavelength of 407 nm was indicated in the present study. Therefore, silver nanoparticles not only maintained their size at around 7 nm, they also were homogenously distributed in film separated only by a silica shell that was twice their thickness. The advantage of this method is that the distance between the silver in core particles can be controlled by the silica thickness.

4. Conclusions

The present study shows that by adjusting the hydrolysis reaction time for TEOS and the initial TEOS concentration, the size of silica-coated silver nanoparticles can be controlled. Theoretical calculation based on the hydrolysis rate of TEOS can accurately predict the size of silica-coated silver nanoparticles for various hydrolysis times and TEOS concentrations. The peak of absorption spectra, as characterized by the surface plasmon resonance (SPR) of the silver nanoparticle dispersant, was at a wavelength of 414 nm, which differed significantly from the peak of silver nanoparticle film at a wavelength of 466 nm. On the other hand, the silica-coated silver nanoparticle dispersant and film were characterized by a similar SPR with peaks of absorption spectra at wavelengths of 407–414 nm. Silica coated on silver nanoparticles maintained the SPR characteristics of the core particles.

Acknowledgements

The authors wish to thank Dr. Eishi Tanabe (Hiroshima Prefectural Inst. Industrial Sci. Tech.) for his TEM analysis and discussions. The Hiroshima Prefecture Institute of Industrial Science and Technology supported this work.

References

[1] K. Okuyama, I.W. Lenggoro, Preparation of nanoparticles via spray route, Chem. Eng. Sci. 58 (2003) 537–547.
[2] L.M. Liz-Marzan, P. Mulvaney, The assembly of coated nanocrystals, J. Phys. Chem. B. 107 (2003) 7312–7326.
[3] L.M. LizMarzan, M. Giersig, P. Mulvaney, Synthesis of nanosized gold-silica core–shell particles, Langmuir 12 (1996) 4329–4335.
[4] L. Armelao, D. Barreca, G. Bottaro, A. Gasparotto, S. Gross, C. Maragno, E. Tondello, Recent trends on nanocomposites based on Cu, Ag and Au clusters: a closer look, Coord. Chem. Rev. 250 (2006) 1294–1314.
[5] P. Mulvaney, Surface plasmon spectroscopy of nanosized metal particles, Langmuir 12 (1996) 788–800.
[6] S.G. Kim, N. Hagura, F. Iskandar, K. Okuyama, Characterization of silica-coated Ag nanoparticles synthesized using a water-soluble nanoparticle micelle, Adv. Powder Technol. 20 (2009) 94–100.
[7] W. Zhang, X. Qiao, J. Chen, Synthesis of silver nanoparticles—effects of concerned parameters in water/oil microemulsion, Mater. Sci. Eng. B-Solid 142 (2007) 1–15.
[8] H. Hiramatsu, F.E. Osterloh, A simple large-scale synthesis of nearly monodisperse gold and silver nanoparticles with adjustable sizes and with exchangeable surfactants, Chem. Mater. 16 (2004) 2509–2511.
[9] X. Liu, M. Atwater, J.H. Wang, Q. Dai, J.H. Zou, J.P. Brennan, Q. Huo, A study on gold nanoparticle synthesis using oleylamine as both reducing agent and protecting ligand, J. Nanosci. Nanotechnol. 7 (2007) 3126–3133.
[10] Z.C. Xu, C.M. Shen, Y.L. Hou, H.J. Gao, S.S. Sun, Oleylamine as both reducing agent and stabilizer in a facile synthesis of magnetite nanoparticles, Chem. Mater. 21 (2009) 1778–1780.
[11] M. Chen, Y.G. Feng, X. Wang, T.C. Li, J.Y. Zhang, D.J. Qian, Silver nanoparticles capped by oleylamine: formation, growth, and self-organization, Langmuir 23 (2007) 5296–5304.
[12] M Giersig, T. Ung, L.M. LizMarzan, P. Mulvaney, Direct observation of chemical reactions in silica-coated gold and silver nanoparticles, Adv. Mater. 9 (1997) 570–575.
[13] W. Stöber, A. Fink, E. Bohn, Controlled growth of monodisperse silica spheres in the micron size range, J. Colloid Interface Sci. 26 (1968) 62–69.
[14] Y. Lu, Y.D. Yin, B.T. Mayers, Y.N. Xia, Modifying the surface properties of superparamagnetic iron oxide nanoparticles through a sol–gel approach, Nano Lett. 2 (2002) 183–186.
[15] L.M. Liz-Marzan, A.P. Philipse, Synthesis and optical properties of gold-labeled silica particles, J. Colloid Interface Sci. 176 (1995) 459–466.
[16] Y. Kobayashi, H. Katakami, E. Mine, D. Nagao, M. Konno, L.M. Liz-Marzan, Silica coating of silver nanoparticles using a modified Stöber method, J. Colloid Interf. Sci. 283 (2005) 392–396.
[17] T. Li, J. Moon, A.A. Morrone, J.J. Mecholsky, D.R. Talham, J.H. Adair, Preparation of Ag/SiO_2 nanosize composites by a reverse micelle and sol–gel technique, Langmuir 15 (1999) 4328–4334.
[18] Y. Han, J. Jiang, S.S. Lee, J.Y. Ying, Reverse microemulsion-mediated synthesis of silica-coated gold and silver nanoparticles, Langmuir 24 (2008) 5842–5848.
[19] C.L. Chang, H.S. Fogler, Controlled formation of silica particles from tetraethyl orthosilicate in nonionic water-in-oil microemulsions, Langmuir 13 (1997) 3295–3307.
[20] S.G. Kim, N. Hagura, F. Iskandar, A. Yabuki, K. Okuyama, Multilayer film deposition of Ag and SiO_2 nanoparticles using a spin coating process, Thin Solid Films 516 (2008) 8721–8725.
[21] D. Nagao, H. Osuzu, A. Yamada, E. Mine, Y. Kobayashi, M. Konno, Particle formation in the hydrolysis of tetraethyl orthosilicate in pH buffer solution, J. Colloid Interface Sci. 279 (2004) 143–149.
[22] W. Wang, S.A. Asher, Photochemical incorporation of silver quantum dots in monodisperse silica colloids for photonic crystal application, J. Am. Chem. Soc. 123 (2001) 12528–12535.
[23] Y. Lu, Y.D. Yin, Z.Y. Li, Y.A. Xia, Synthesis and self-assembly of $Au@SiO_2$ core–shell colloids, Nano Lett. 2 (2002) 785–788.
[24] S.J. Oldenburg, R.D. Averitt, S.L. Westcott, N.J. Halas, Nanoengineering of optical resonances, Chem. Phys. Lett. 288 (1998) 243–247.
[25] L. Armelao, R. Bertoncello, M. DeDominicis, Silver nanocluster formation in silica coatings by the sol–gel route, Adv. Mater. 9 (1997) 736–741.